# Laser-induced fluorescence measurements of argon and xenon ion velocities near the sheath boundary in 3 ion species plasmas

Chi-Shung Yip,[1] Noah Hershkowitz,[1] Greg Severn,[2] and Scott D. Baalrud[3]
[1]*Department of Engineering Physics, University of Wisconsin-Madison, Madison, Wisconsin 53706, USA*
[2]*Department of Physics, University of San Diego, San Diego, California 92110, USA*
[3]*Department of Physics and Astronomy, University of Iowa, Iowa City, Iowa 52242, USA*

(Received 9 April 2016; accepted 3 May 2016; published online 13 May 2016)

The Bohm sheath criterion is studied with laser-induced fluorescence in three ion species plasmas using two tunable diode lasers. Krypton is added to a low pressure unmagnetized DC hot filament discharge in a mixture of argon and xenon gas confined by surface multi-dipole magnetic fields. The argon and xenon ion velocity distribution functions are measured at the sheath-presheath boundary near a negatively biased boundary plate. The potential structures of the plasma sheath and presheath are measured by an emissive probe. Results are compared with previous experiments with Ar–Xe plasmas, where the two ion species were observed to reach the sheath edge at nearly the same speed. This speed was the ion sound speed of the system, which is consistent with the generalized Bohm criterion. In such two ion species plasmas, instability enhanced collisional friction was demonstrated [Hershkowitz *et al.*, Phys. Plasmas **18**(5), 057102 (2011).] to exist which accounted for the observed results. When three ion species are present, it is demonstrated under most circumstances the ions do not fall out of the plasma at their individual Bohm velocities. It is also shown that under most circumstances the ions do not fall out of the plasma at the system sound speed. These observations are also consistent with the presence of the instabilities. *Published by AIP Publishing.*
[http://dx.doi.org/10.1063/1.4950823]

In a multi ion species plasma, ions at the sheath-presheath boundary must satisfy[1,2]

$$1 \geq \sum_j (n_j c_j^2)/(n_e v_j^2), \tag{1}$$

where $v_j$ is the velocity of each ion species at the sheath edge, $c_j$ is the individual Bohm velocity $(T_e/m_j)^{1/2}$ of each ion species, and $n_j/n_e$ is the relative ion concentration. $T_e$ and $m_j$ are the electron temperature and the mass of ion species j, respectively. Equation (1) encompasses a general ion flow at the sheath-presheath boundary and we refer to it as the generalized Bohm Criterion (GBC).[3] Previous experiments had demonstrated that in a weakly collisional, two ion species plasma, the GBC, is satisfied.[4]

In the research literature, the term "generalized Bohm Criterion" has two distinct usages. The oldest usage stems from the original kinetic theory generalization of Bohm's criterion by Harrison and Thompson,[5] referring to a single ion species plasma. The first such reference belongs to Allen.[6] A second usage comes in about the same time as Riemann's pioneering work on the multicomponent plasmas (Eq. (1)), which Reimann did not refer to as the generalized Bohm Criterion. Valentini and Herrmann did[7] a year later, and we have adopted this usage in our work.[3] Valentini and Herrmann and Riemann pointed out that the theory and science of sheath formation is important in all bounded plasma systems, and that nearly all applications of plasma physics involve this important feature (e.g., gas discharge lamps, gas lasers, plasma processing applications such as wafer processing in Ultra large-scale integration, and plasma-surface interactions in controlled nuclear fusion, even astrophysical applications). Yet despite being one of the oldest problems in plasma physics, sheath formation is still not fully understood. This is demonstrated by the work described in this paper, which is the first to give an account of sheath formation and the GBC in the multicomponent ion plasmas in which there are more than two species of positive ions. We found an unexpected feature of ion speeds at the sheath edge when there are 3 positive ion species: under most circumstances the ions do not fall out of the plasma at the system sound speed or their individual Bohm speeds. This is the principal result of this paper.

When $T_e \gg T_i$, with two ion species, there is a continuum of solutions to the GBC. The two simplest solutions are that ions travel at their individual Bohm velocities[8] or that the ions travel at a system sound velocity, which is the ion acoustic velocity in the bulk plasma, $c_s = \sqrt{\sum_j (n_j k_B T_e)/n_e m_j}$ where $k_B$ is the Boltzmann constant. However, the GBC has been shown experimentally to be satisfied with both ion species travelling close to the system sound velocity $c_s$ when the ion densities are comparable and at their individual Bohm velocities when one ion species dominates.[4,9–12] A recent theory argued that ion-ion two stream instabilities were responsible for such phenomena.[13–15]

Experiments were performed in a 60 cm diameter, 70 cm long multi-dipole chamber as shown schematically in Figure 1. The chamber is surrounded by 12 rows of magnets with alternating poles on its cylindrical surface. The base vacuum of the chamber is approximately $5 \times 10^{-7}$ Torr. Plasma was produced through impact ionization by energetic primary electrons provided by three sets of 9 filaments installed on one end wall of the chamber. The filaments were biased at −60 V with respect to the grounded chamber and were

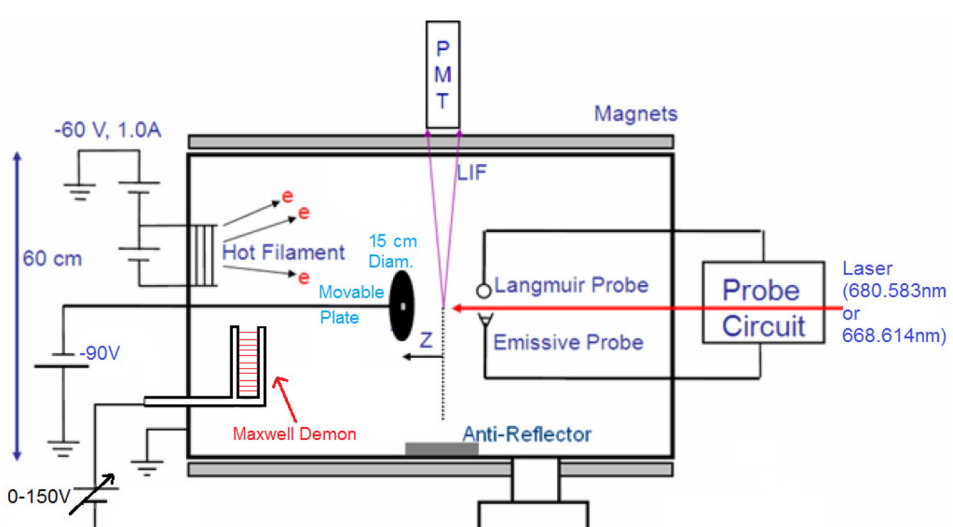


FIG. 1. A schematic drawing of the multi-dipole chamber setup. The locations of the Langmuir probe, emissive probe, Maxwell Demon, PMT, and the movable plate electrode are shown.

ohmically heated to emit electrons. In this work, the current of primary electrons $I_{pri}$ was $1.00 \pm 0.03$ A. Primary electrons are accelerated through the sheath surrounding the filaments usually a few mm thick, and essentially retain their energy until impacts with neutrals occur. Primary electrons are well confined by the multi-dipole field such that they are more likely to be lost due to ionization than by the impact with the wall. This generates a very uniform plasma throughout the device with no spatial inhomogeneities nor any anisotropy in the velocity of the ions in the bulk plasma which is far from the filaments. A movable 15 cm diameter stainless steel plate is biased at $-90$ V to form a thick sheath and its corresponding presheath to be studied. A MacKenzie's Maxwell Demon is employed on the filament side of the chamber to control the electron temperature $T_e$ for the study.[16,17]

A movable 0.64 cm diameter tantalum Langmuir probe was employed at the axis of the chamber to measure the bulk electron density $n_e$ and the electron temperature $T_e$. A cylindrical emissive probe made of a 0.025 mm diameter, 5 mm long tungsten filament was employed using the inflection point technique in the limit of zero emission to measure the local plasma potential throughout the presheath.[18] The emissive probe was also used to determine the location of the sheath-presheath boundary by observing the change of slope of the inflection points.[19,20] The system sound velocity $c_s$ was determined by ion acoustic wave (IAW) phase velocity measurements of a continuous wave launched from a 10 cm diameter grid. The wave was detected with a negatively biased 0.64 cm diameter Langmuir probe swept axially and the direct coupled signal filtered with a boxcar averager.[21]

In this study, argon and xenon neutral pressures were set at 0.1 mTorr and 0.04 mTorr, respectively. The neutral pressure mixture corresponded to an approximately 50–50 mixture of the two ion species as determined by the IAW phase velocity. Krypton gas was gradually added to the system to change the relative concentration of the three ion species. It is important to note that the relative neutral gas concentrations do not equal the relative ion concentrations due to the differences in ionization cross sections and Penning ionizations, among other effects.

With two ion species plasmas, the relative ion concentrations can be determined from the IAW phase velocity.[22] However, with three ion species, the IAW dispersion relation no longer determines a solution of the 3 ion concentrations. A crude estimation of the krypton relative ion density is to assume that the argon and xenon relative ion densities stay constant proportional to each other as the third gas is added to the system. This gives us a rough approximation of how the drift velocities of the third ion species at the sheath edge change with the ion concentrations by assuming the GBC. Because we do not have the LIF schemes working for all three ion species, we cannot experimentally test the GBC in this work.

Two tunable diode lasers were employed to perform the LIF measurements of Ar+ and Xe+ ion velocity distribution functions (ivdfs). To obtain Xe II LIF, a laser with its wavelength centered at 680.580 nm (in air) was finely tuned over a 10 GHz range to excite the xenon ions in the metastable state $5p^4(^3P_1)5d[3]_{7/2}$ to the $5p^4(^3P_1)6p[2]^0_{5/2}$ state, leading to the spontaneous emission at 492.15 nm wavelength (air) and the decay to the $5p^4(^3P_1)6s[1]_{3/2}$ state. To obtain Ar II LIF, another laser with its wavelength centered at 668.614 nm (vacuum) was finely tuned over a 10 GHz range to excite argon ions in the metastable state $4s^4P_{3/2}$ to the excited $4p^4D^0_{5/2}$ state which immediately fluoresces at 442.6 nm (vacuum) as the ion decay to the $3d^4F_{7/2}$ state. A photomultiplier tube (PMT) and a collection optics composed of two lenses were fixed on top of the chamber as shown in Figure 1. The 15 cm diameter plate was moved along the axis of the chamber to measure ivdfs as a function of position from the plate. A schematic of the laser setup is shown in Figure 2.

We performed experiments in a $T_e = 1.95 \pm 0.08$ eV, 0.1 mTorr argon and 0.04 mTorr xenon plasma with krypton progressively added into the plasma. Without adding krypton, the xenon and argon relative ion concentrations $n_j/n_e$ were both measured to be $50 \pm 5\%$ through solving the dispersion relationship of the IAW with the measured IAW phase velocity and $T_e$ measured by the Langmuir probe. At this relative

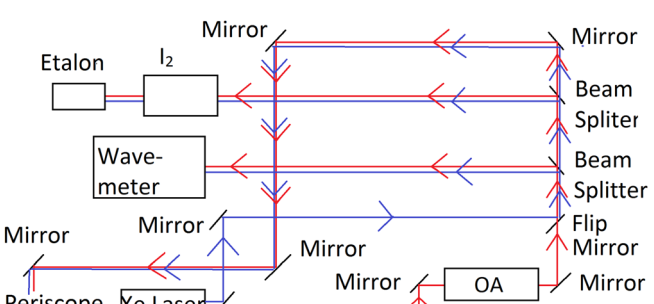


FIG. 2. Schematic diagram of the laser setup. The Ar laser beam passes through a tapered chip optical amplifier (OA) to increase the laser power. An iodine cell provides a known fluorescence spectrum with features to identify absolute wavelength. This is combined with the etalon which provides a direct measurement of detuning. A wavemeter is used for coarse tuning to the excitation line.

ion concentration of xenon and argon, both ion species drifted close to the system sound speed at the sheath-presheath boundary, as previously predicted and measured.[12,13]

Figure 3 shows the change of ion drift velocities and $c_s$ at the sheath-presheath boundary as krypton neutral pressure was increased. When the krypton concentration was relatively low, the drift velocities of xenon and argon ions were close to system sound velocity $c_s$, as with the case when krypton ions were absent. As krypton neutral pressure increased, both argon and xenon ions drift velocities separated and eventually approached their individual Bohm velocities. Since krypton's ion mass is between the argon and xenon ion masses, $c_s$ was close ($\sim$300 m/s) to the krypton individual Bohm velocity even without krypton ions. As the krypton neutral pressure increased, $c_s$ became even closer to the individual Bohm velocity of the krypton ions.

At low krypton concentration, the krypton ion drift velocity is expected to be faster than or equal to its own Bohm velocity. This expectation is based on the argument that at low concentration no interactions between the three ion species are available to cause the krypton ions to be accelerated faster than the lighter species or to be decelerated

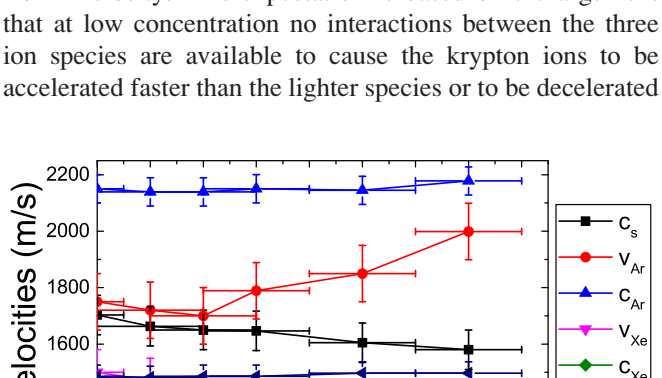


FIG. 3. Measured Ar+ and Xe+ ion drift velocities at the sheath-edge. Ar+, Xe+, and Kr+ individual Bohm velocities calculated from the measured electron temperature, and the measured system sound velocity $c_s$ is graphed versus the krypton neutral pressure. For all data points in this figure, $T_e = 1.95 \pm 0.08$ eV, and argon and xenon neutral pressures are fixed at 0.1 mTorr and 0.04 mTorr respectively.

slower than the heavier species. At high krypton concentration, argon and xenon drift close to their individual Bohm velocities, thus the krypton ion drift velocity is required to be close to its individual Bohm velocity, which is also close to $c_s$, by the GBC.

According to the instability enhanced collisional friction theory[13–15] applied to two-ion species plasmas, ion-ion two-stream instability can onset as the lighter species obtain sufficiently faster speed than the heavier species in response to the presheath electric field. After onset, a strong friction force arises between the ion species that is associated with the wave particle scattering. The associated friction force is sufficiently strong that it prevents the differential flow speed between ion species from significantly exceeding the threshold condition for two-stream instability. This pulls the drift velocities of the two ion species closer together, so that they no longer exit the plasma at their individual Bohm velocities in general. The instabilities may also lead to the nonlinear trapping of ions that could influence local velocity structure of the ivdfs. In order for two-stream instability to occur, the total ivdf is required to have a minimum velocity gap between the two ion species. This implies an ion concentration dependence on the threshold condition for instability onset, which led to the prediction that ions obtain a speed near the system sound speed when the mix is near 50–50, and near the individual sound speeds for dilute concentrations.[13,14] This was confirmed experimentally.[4,12]

Here, adding krypton to the system introduces ions with drift velocities between the argon and xenon populations. As the krypton ion concentration increases, it fills the gap in velocity space of the total ivdf and raises the threshold differential flow between argon and xenon at which the instability onsets. At sufficiently large krypton ion concentration, the instability will be completely suppressed. This leads to the prediction that argon and xenon ions will have speeds near the system sound speed at low krypton concentration, and will trend toward their individual sound speeds as the krypton concentration increases, eventually reaching these speeds at sufficiently large krypton concentration.

A comprehensive quantitative comparison between theory and experiment is not possible without a measurement of the concentration of each species, and a direct measurement of the krypton ion speed. However, a qualitative comparison between the measurements and the theoretical expectation that the argon and xenon ion speeds transition from near the system sound speed at dilute krypton concentrations to approaching their individual sounds speeds as the krypton concentration increases was made as follows: The threshold conditions for instability were estimated from the dispersion relation obtained by solving for the roots of the linear dielectric response function for ion-frequency fluctuations where $\frac{\omega}{v_{Te}k} \ll 1$,[15,23]

$$\hat{\varepsilon} = 1 + \frac{1}{k^2\lambda_{De}^2}\left[1 - \frac{1}{2}\sum_{j=1}^{3}\frac{T_e}{T_j}x_j Z'(\xi_j)\right], \qquad (2)$$

in a manner similar to what was done for two ion species.[15] Here, $x_j = n_j/n_e$ is the relative concentration of species $j$,

$\lambda_{De}$ is the electron Debye length, $Z'$ is the first derivative of the plasma dispersion function, and $\xi_j = (\omega - kV_j)/kv_{Tj}$ where $v_{Tj} = \sqrt{2k_BT_j/m_j}$. In the following, argon, krypton, and xenon ions are labeled as species 1, 2, and 3, respectively.

The critical flow difference between argon and xenon, $\Delta V_{13} = V_1 - V_3$, at which the instability onset was obtained directly from Eq. (2) in the following manner. First, the substitution $\omega = \frac{1}{2}k(V_1 + V_3) + k\Delta V_{13}\Omega$ was applied, which defines the variable $\Omega$. The advantage of this is that the growth rate can be determined by the differential flow speeds $\Delta V_{13}$ and $\Delta V_{12}$ rather than the speed of each of the three species individually. Equation (2) was then solved iteratively for the minimum $\Delta V_{13}$ at which instability onsets (by determining the value for which $\max\{\gamma(k)\} = 0$, where $\gamma = \mathrm{Im}\{\omega\}$ is the growth rate). This is required setting a value for $\Delta V_{12}$. The main approximation made was that krypton has its individual sound speed at the sheath edge ($V_2 = c_{s2}$), independent of concentration. This is an estimate motivated by an argument that the instability enhanced friction influences the species responsible for the two-stream instability (argon and xenon), but not the "passive" species (krypton). However, we emphasize that this is a simple approximation that has been made to make progress on understanding the qualitative features of the data. It is not a rigorous theoretical prediction and it has not been tested experimentally. With this approximation, Equation (1) was solved for $\Delta V_{12}$ in terms of $\Delta V_{13}$, $V_2$ and the masses and concentrations of the ion species. This value was then used in the stability analysis to obtain the threshold $\Delta V_{13}$ at fixed concentrations. The processes were then repeated as the krypton concentration was varied, subject to the constraint that $x_1 + x_2 + x_3 = 1$ and assuming that the argon and xenon ions were present in equal concentrations ($x_1 = x_3$). In general, it was found that there were two possible unstable modes. The mode with the lowest threshold $\Delta V_{13}$ at any concentration was selected. Finally, this solution for $\Delta V_{13}$ was used along with Eq. (1) to determine the speed of each ion species $(V_1, V_2, V_3)$ at the sheath edge.

Figure 4 compares the experimentally measured velocities with predictions made assuming ions had a temperature equal to the measured ion temperature of $0.03 \pm 0.005$ eV in the bulk. Data are graphed versus an estimated relative krypton ion concentration that assumes equal ion concentrations between argon and xenon ions, i.e., $n_{Ar}/n_{Xe} = 1$ as krypton gas is added. The IAW phase velocity $c_s = \sqrt{\sum_j (n_j k_B T_e)/n_e m_j}$ is then solved using the measured $T_e$ to extract the relative krypton ion concentration. The predictions provided agreement with the measured Xe+ ion drift velocities and showed the qualitative features of the measured Ar+ ion drift velocities. The feature that the argon and xenon drift velocity at the sheath edge changed from near the system sound speed toward their individual sound speeds as the krypton concentration increased is apparent in both the experimental data and theoretical prediction. A quantitative comparison is not justified since the theory made significant assumptions regarding the krypton speed and also assumed that the argon and xenon concentrations remain equal as krypton is added to the system. These features could not be measured experimentally.

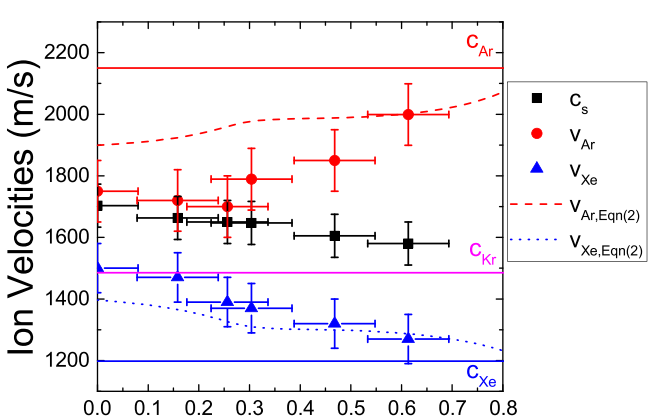


FIG. 4. Measured Ar+ and Xe+ drift velocities at the sheath-edge. Ar+, Xe+, and Kr+ individual Bohm velocities calculated from the measured $T_e = 1.95 \pm .08$ eV, and the measured system sound velocity $c_s$ are graphed versus the estimated Kr+ relative ion concentration. Predicted velocities of Ar+ and Xe+ ions with $T_i = 0.03$ eV are labelled as $v_{Ar,Eqn(2)}$ and $v_{Xe,Eqn(2)}$ and graphed as dashed and dotted lines, respectively.

For the first time, the drift velocities of two ion species at the sheath-presheath boundary of three ion species plasmas were measured. It is demonstrated that under most circumstances the ions do not fall out of the plasma at their individual Bohm velocities, as had previously been assumed in most investigations. It is also shown that under most circumstances the ions do not fall out of the plasma at the system sound speed. It is found that if an additional third ion species was added to a two ion species plasma in which the ions were drifting close to the system sound velocity at the sheath-presheath boundary, the drift velocities of the two ion species return close to their individual Bohm velocities as the concentration of the third ion species increases. This is consistent with the theory of instability enhanced collisional friction that if the instability is turned off, ions will exit the plasma close to their individual Bohm velocities.

This work was supported by NSF under Grant No. 1464741 and U.S. DOE under Grant No. DE-SC00114226.

[1]M. J. Cook, "Properties of optically pumped discharges," Ph.D. thesis, University of Oxford, 1980.
[2]K. U. Riemann, IEEE Trans. Plasma Sci. **23**(4), 709–716 (1995).
[3]G. D. Severn, X. Wang, E. Ko, and N. Hershkowitz, Phys. Rev. Lett. **90**(14), 145001 (2003).
[4]N. Hershkowitz, C. S. Yip, and G. D. Severn, Phys. Plasmas **18**(5), 057102 (2011).
[5]E. R. Harrison and W. B. Thompson, Proc. Phys. Soc. **74**(2), 145 (1959).
[6]J. E. Allen, J. Phys. D: Appl. Phys. **9**(16), 2331 (1976).
[7]H. B. Valentini and F. Herrmann, J. Phys. D: Appl. Phys. **29**(5), 1175 (1996).
[8]R. N. Franklin, J. Phys. D: Appl. Phys. **33**(24), 3186–3189 (2000).
[9]N. Hershkowitz, E. Ko, X. Wang, and A. M. A. Hala, IEEE Trans. Plasma Sci. **33**(2), 631–636 (2005).
[10]D. Lee, N. Hershkowitz, and G. D. Severn, Appl. Phys. Lett. **91**(4), 041505 (2007).
[11]D. Lee, L. Oksuz, and N. Hershkowitz, Phys. Rev. Lett. **99**(15), 155004 (2007).
[12]C.-S. Yip, N. Hershkowitz, and G. Severn, Phys. Rev. Lett. **104**(22), 225003 (2010).

[13]S. D. Baalrud and C. C. Hegna, Phys. Plasmas **18**(2), 023505 (2011).
[14]S. D. Baalrud, C. C. Hegna, and J. D. Callen, Phys. Rev. Lett. **103**(20), 205002 (2009).
[15]S. D. Baalrud, T. Lafleur, W. Fox, and K. Germaschewski, Plasma Sources Sci. Technol. **24**(1), 015034 (2015).
[16]C.-S. Yip, J. P. Sheehan, N. Hershkowitz, and G. Severn, Plasma Sources Sci. Technol. **22**(6), 065002 (2013).
[17]K. R. MacKenzie, R. J. Taylor, D. Cohn, E. Ault, and H. Ikezi, Appl. Phys. Lett. **18**(12), 529 (1971).
[18]J. R. Smith, N. Hershkowitz, and P. Coakley, Rev. Sci. Instrum. **50**(2), 210–218 (1979).
[19]J. P. Sheehan, Y. Raitses, N. Hershkowitz, I. Kaganovich, and N. J. Fisch, Phys. Plasmas **18**(7), 073501 (2011).
[20]X. Wang and N. Hershkowitz, Rev. Sci. Instrum. **77**(4), 043507 (2006).
[21]L. Oksuz, D. Lee, and N. Hershkowitz, Plasma Sources Sci. Technol. **17**(1), 015012 (2008).
[22]A. M. Hala and N. Hershkowitz, Rev. Sci. Instrum. **72**(5), 2279–2281 (2001).
[23]D. G. Swanson, *Plasma Waves*, 2nd ed. (Taylor & Francis, 2003).